If U_i is much less than $\chi^2 + U_r$, then α and β can be approximated as

$$\alpha = (\chi^2 + U_r)^{1/2}[1 + \tfrac{1}{8}(U_i^2/U_r^2)], \quad (A4a)$$

$$\beta = U_i/2(\chi^2 + U_r)^{1/2}. \quad (A4b)$$

The reflected amplitude, R, can be solved by matching the boundary conditions.

$$R = (\chi - \alpha - i\beta)/(\chi + \alpha + i\beta). \quad (A5)$$

In the limit of small K or for $\chi^2 < U_r$, the reflected amplitude is unity. For large χ (corresponding to a large angle for the specular beam) it can be approximated as

$$R = iU_i/4\chi^2, \quad (A6)$$

which only depends strongly on the imaginary part of the potential. The reflected intensity is therefore

$$I = U_i^2/16\chi^4. \quad (A7)$$

References

BETHE, H. (1928). *Ann Phys. (Leipzig)*, **87**, 55–69.
BIRD, D. M. & KING, Q. A. (1990). *Acta Cryst.* A**46**, 202–208.
COHEN, P. I., PETRICH, G. S., PUKITE, P. R., WHALEY, G. J. & ARROTT, A. S. (1989). *Surf. Sci.* **216**, 222–248.
COLELLA, R. (1972). *Acta Cryst.* A**28**, 11–15.
DOYLE, P. A. & TURNER, P. S. (1968). *Acta Cryst.* A**24**, 390–397.
DUDAREV, S. L. & WHELAN, M. J. (1994). *Phys. Rev. Lett.* **72**, 1032–1035.
FATHERS, D. J. & REZ, P. (1979). *Scanning Electron Microscopy* 1, pp. 55–66. O'Hare: SEM Inc.
FATHERS, D. J. & REZ, P. (1984). *Electron Beam Interactions with Solids*, pp. 193–208. O'Hare: SEM Inc.
HIRSCH, P. B., HOWIE, A., WHELAN, M. J., NICHOLSON, R. B. & PASHLEY, D. W. (1965). *Electron Microscopy of Thin Crystals*. London: Butterworths.
ICHIMIYA, A. (1983). *Jpn. J. Appl. Phys.* **22**, 176–180.
ICHIMIYA, A. (1990). *Surf. Sci.* **235**, 75–83.
KNIBB, M. G. (1991). *Surf. Sci.* **257**, 389–401.
KOHRA, K. & SHINOHARA, K. (1948). *J. Phys. Soc. Jpn*, **4**, 155–160.
KORTE, U. & MEYER-EHMSEN, G. (1993). *Phys. Rev. B*, **48**, 8345–8355.
MA, Y., LORDI, S., LARSEN, P. K. & EADES, J. A. (1993). *Surf. Sci.* **289**, 47–67.
MAKSYM, P. A. & BEEBY, J. L. (1981). *Surf. Sci.* **110**, 423–438.
MEYER-EHMSEN, G. (1989). *Surf. Sci.* **219** 177–188.
MOON, A. R. (1972). *Z. Naturforsch.* **27**, 391–395.
NEAVE, J. H., DOBSON, P. J., JOYCE, B. A. & ZHANG, J. (1985). *Appl. Phys. Lett.* **47**, 100–102.
PENG, L.-M. & COWLEY, J. M. (1986). *Acta Cryst.* A**42**, 545–552.
PENG, L.-M. & DUDAREV, S. L. (1993). *Surf. Sci.* **298**, 316–330.
PENG, L.-M. & WHELAN, M. J. (1990). *Proc. R. Soc. London Ser. A*, **431**, 125–142.
PENG, L.-M. & WHELAN, M. J. (1991*a*). *Acta Cryst.* A**47**, 95–101.
PENG, L.-M. & WHELAN, M. J. (1991*b*). *Proc. R. Soc. London Ser. A*, **432**, 195–213.
PENG, L.-M. & WHELAN, M. J. (1991*c*). *Proc. R. Soc. London Ser. A*, **435**, 257–267.
PENG, L.-M. & WHELAN, M. J. (1991*d*). *Proc. R. Soc. London Ser. A*, **435**, 269–286.
PENG, L.-M. & WHELAN, M. J. (1992). *Surf. Sci. Lett.* **268**, L325–L329.
STOCK, M. & MEYER-EHMSEN, G. (1990). *Surf. Sci. Lett.* **226**, L59–L62.
YAGI, K. (1987). *J. Appl. Cryst.* **20**, 147–160.
ZHAO, T. C., POON, H. C. & TONG, S. Y. (1988). *Phys. Rev. B*, **38**, 1172–1195.
ZUO, J. M. & LIU, J. (1992). *Surf. Sci.* **271**, 253–259.

Acta Cryst. (1995). A**51**, 47–53

On the Single-Pixel Approximation in Maximum-Entropy Analysis

BY SHINTARO KUMAZAWA

Department of Physics, Science University of Tokyo, Chiba, 278 *Japan*

AND MASAKI TAKATA AND MAKOTO SAKATA

Department of Applied Physics, Nagoya University, Nagoya, 464 *Japan*

(*Received* 21 *June* 1993; *accepted* 31 *May* 1994)

Abstract

By a recent development of the maximum-entropy method (MEM) following Sakata & Sato [*Acta Cryst.* (1990), A**46**, 263–270], electron- (or nuclear-) density distributions have been obtained for crystalline materials of simple structures from single-crystal or powder diffraction data. In order to obtain a ME density map, the ME equation is solved iteratively under the zeroth-order single-pixel approximation (ZSPA) starting from the uniform density. The purpose of this paper is to examine the validity of the ZSPA by using a one-dimensional two-pixel model for which the exact solution can be analytically obtained. For this model, it is also possible to solve the ME equation numerically without ZSPA by the same iterative procedure as in the case of ZSPA. By comparison of these three solutions for a one-

dimensional two-pixel model, it is found that the solutions obtained iteratively both with and without ZSPA always converge to the exact solution so long as the value of the Lagrange undetermined multiplier, λ, is chosen to be sufficiently small. This means the ZSPA solution does not depend on λ when the convergence is attained. When λ exceeds a critical value, iteration with ZSPA gives oscillatory divergence but iteration without ZSPA converges to a different value from the exact solution. It is concluded that the introduction of ZSPA does not cause any serious problem in the solution of the ME equation, when a sufficiently small λ value is used in the ME analysis.

1. Introduction

Recently, a new method has been developed in the field of accurate structure analysis to obtain electron- (or nuclear-) density distributions from X-ray (or neutron) diffraction data. It utilizes the maximum-entropy method (MEM) in order to restore the electron (or nuclear) densities of crystalline materials from observed structure-factor data (Sakata & Sato, 1990). The superiority of the ME density map over the conventional Fourier map is very clearly shown in some cases (Sakata & Sato, 1990; Sakata, Mori, Kumazawa, Takata & Toraya, 1990; Sakata, Uno, Takata & Howard, 1993). The MEM can be applied in the case where only a limited number of observed structure factors are available, such as in a powder diffraction experiment. The number of examples in which the ME analysis has been successfully applied to the accurate determination of electron (or nuclear) densities is now rapidly increasing.

The purpose of these studies is to restore, in the form of electron- or nuclear-density distributions, as much as possible of the structural information included in accurately determined structure factors of simple materials. This is surely one of the frontiers of accurate structure analysis. For such a purpose, the ME equation, which is mathematically a transcendental equation, has so far been solved by an iterative method under the following conditions: (1) satisfaction of the symmetry requirements of the crystals; (2) conservation of the total number of electrons (or nuclei) in a unit cell; (3) use of the zeroth-order single-pixel approximation (ZSPA) in order to solve the MEM equation. The iteration starts from the uniform density because it corresponds to the state of maximum entropy when there is no structural information. In this way, any prejudice in choosing the initial density for the iteration can be excluded, which has essential importance for the problem mentioned above. When the MEM is applied to some other purposes, such as the phase problem (*e.g.* Bricogne & Gilmore, 1990; Gilmore, Bricogne & Bannister, 1990), the procedure described above may not be appropriate.

The first and second conditions are necessary to make the ME density map consistent with the crystallographic knowledge. It is very reasonable to consider that these conditions must be compulsorily satisfied. The third condition is, however, helpful for mathematical reasons. For this purpose, Wilkins, Varghese & Lehmann (1983) introduced the single-pixel approximation. On the other hand, we employ the ZSPA and thus the ME equation becomes a simple linear equation and solvable in an iterative way. The results of the ME analysis so far obtained under the ZSPA seem to be physically and chemically acceptable as electron (or nuclear) densities of materials; for example, the nature of chemical bonding of the specimen, such as covalency, is reproduced in the form of electron densities. Hence, the validity of the ZSPA has been taken as granted without any theoretical considerations. It is not known what kind of influence failure of the ZSPA would have on the solution of the ME equation. It is therefore very important to examine the validity and limitation of the ZSPA on a theoretical basis, not only in order to establish the ME analysis in crystallography but also for basic understanding of the MEM.

In this paper, an extremely simple case of a one-dimensional two-pixel model is considered. This model has no reality as a practical crystal. From a theoretical viewpoint, however, this is a very interesting and valuable model. First of all, the exact solution of the ME equation can be analytically derived; secondly, the iterative solution can be obtained by calculating the Lagrangian numerically without using the ZSPA. Therefore, this model is most suitable for the purpose of the present paper, which is to examine the validity of the ZSPA when it is used to calculate the ME density map.

2. Theory

The theoretical background of ME analysis is briefly mentioned in order to explain the ZSPA. The present ME formalism is essentially based on the work of Collins (1982), in which the ME equation was derived under the approximation that neglects a term of reciprocals of the squared density distribution. Sakata, Uno, Takata & Mori (1992) later showed that the same equation can be derived without introducing the approximation by taking the differential for the maximum condition of the Lagrangian with respect to the normalized densities instead of the real densities. In order to avoid unnecessary complexity in deriving the ME equation, the theory is given here for the X-ray case. It is fairly straightforward to rewrite the equations to suit the neutron diffraction case if there is no negative-scattering-density prob-

lem. The negative-scattering-density problem has been solved by Sakata, Uno, Takata & Howard (1993).

The information-theoretic entropy is written as

$$S = -\sum_{k=0}^{N-1} \rho_k \log(\rho_k/\tau_k), \quad (1)$$

where ρ_k and τ_k are the normalized density and normalized prior density, respectively, at the position $\mathbf{r}_k$ and N is the total number of pixels in the unit cell. The structure-factor and total-charge constraint functions, C and D, are written as

$$C = (1/M)\sum_{j=1}^{M} (1/\sigma_j^2)|F_{\rm calc}(\mathbf{h}_j) - F_{\rm obs}(\mathbf{h}_j)|^2 \quad (2)$$

and

$$D = \sum_{k=0}^{N-1} \rho_k, \quad (3)$$

respectively. In (2), M is the number of known phased structure factors, $F_{\rm obs}(\mathbf{h}_j)$ is the observed structure factor for reflection $\mathbf{h}_j$, σ_j is the standard deviation of $F_{\rm obs}(\mathbf{h}_j)$ and $F_{\rm calc}(\mathbf{h}_j)$ is the calculated structure factor given as

$$F_{\rm calc}(\mathbf{h}_j) = V\sum_{k=0}^{N-1} Q_k \exp(2\pi i \mathbf{h}_j \cdot \mathbf{r}_k), \quad (4)$$

where V is the unit-cell volume and Q_k is the number of electrons at the position $\mathbf{r}_k$. Q_k is defined by $(Q/V)\rho_k$ and Q is the total number of electrons.

When the constraints are satisfied, these functions become 1, because $C=1$ is the expected value of the χ^2-type distribution and $D=1$ shows the total charge of normalized density. Using the Lagrange method of undetermined multipliers, we have the Lagrangian as

$$H(\rho;\lambda,\mu) = S - \lambda[C(\rho)-1] - \mu[D(\rho)-1], \quad (5)$$

where λ and μ are the Lagrange undetermined multipliers for the structural and total-charge constraints, respectively. By setting

$$\partial H/\partial\rho_k = -\log\rho_k - 1 + \log\tau_k - \mu - \lambda(\partial C/\partial\rho_k) = 0, \quad (6a)$$

$$\partial H/\partial\mu = \sum_{k=0}^{N-1} \rho_k - 1 = 0 \quad (6b)$$

and

$$\partial H/\partial\lambda = C - 1 = 0 \quad (6c)$$

for the maximum condition of the Lagrangian, we have the ME equations as

$$\rho_k = \tau_k \exp\left(-\lambda\frac{\partial C}{\partial\rho_k}\right) \Big/ \sum_{k'=0}^{N-1} \tau_{k'} \exp\left(-\lambda\frac{\partial C}{\partial\rho_{k'}}\right) \quad (7)$$

from (6*a*) and (6*b*) and

$$(1/M)\sum_{j=1}^{M} (1/\sigma_j^2)|F_{\rm calc}(\mathbf{h}_j) - F_{\rm obs}(\mathbf{h}_j)|^2 - 1 = 0 \quad (8)$$

from (6*c*). If the normalized densities in (6) are used for the maximum condition, the ME equation can be derived without any approximation (Sakata, Uno, Takata & Mori, 1992).

A problem in obtaining the ME density map is that the ME equation cannot be solved analytically in practical cases, because ρ_k is included on both sides of (7). One way to solve the ME equation is to introduce an approximation. Wilkins, Varghese & Lehmann (1983) introduced the single-pixel approximation. It can be described in two steps. First, the derivative term of the ME equation is expanded in a Taylor series,

$$\frac{\partial C}{\partial\rho_k} = \left[\frac{\partial C}{\partial\rho_k}\right]_{\rho k=\tau k} + \sum_{k=k'} (\rho_{k'} - \tau_{k'}) \left[\frac{\partial^2 C}{\partial\rho_k \partial\rho_{k'}}\right]_{\rho k=\tau k}. \quad (9)$$

Second, only the $k=k'$ term is included in the summation of the second term of (9). Then, the approximated nonlinear single-pixel equation is solved by Newton's method.

The additional assumption of the ZSPA is to ignore all of the second term of (9), which is equivalent to replacing ρ_k by τ_k in the calculation of the structure factor, *i.e.*

$$F_{\rm calc}(\mathbf{h}_j) = V\sum_{k=0}^{N-1} T_k \exp(2\pi i \mathbf{h}_j \cdot \mathbf{r}_k), \quad (10)$$

where T_k is defined by $(Q/V)\tau_k$. By (10), the right-hand side of (7) becomes independent of ρ_k. Therefore, the approximated ME equation can be solved without nonlinearity, although an iteration must still be carried out until the constraint function, (8), is satisfied. In the calculation, the initial density distribution is chosen as uniform, which corresponds to the maximum-entropy state when there is no structural constraint. The value of λ is chosen sufficiently smaller than the exact value. The reason for this is given in §5.

3. One-dimensional two-pixel model

In this section, a one-dimensional two-pixel model is described. An example of the model is shown in Fig. 1. As is seen from the figure, this system always has a center-of-symmetry operation and hence the structure factors are always real. Since only two pixels exist, only two structure factors are necessary to define the complete system. In the present case, we may choose the total charge, $F_{\rm calc}(0)$, and the first-order Fourier coefficient, $F_{\rm calc}(1)$ written as

$$F_{\rm calc}(0) = \rho_0 + \rho_1 \quad \text{and} \quad F_{\rm calc}(1) = \rho_0 - \rho_1, \quad (11)$$

respectively. In order to simplify the expression, it is assumed that $Q=1$ and $V=1$.

For the one-dimensional two-pixel model, (7) and (8) are written as follows:

$$\rho_0 = \tau_0 \exp(\mp 2\lambda/\sigma)/[\tau_0 \exp(\mp 2\lambda/\sigma) + \tau_1 \exp(\pm 2\lambda/\sigma)],$$
$$\rho_1 = \tau_1 \exp(\pm 2\lambda/\sigma)/[\tau_0 \exp(\mp 2\lambda/\sigma) + \tau_1 \exp(\pm 2\lambda/\sigma)] \quad (12)$$

and

$$[(\rho_0 - \rho_1 - F_{obs})^2/\sigma^2] - 1 = 0. \quad (13)$$

By substituting (12) into (13), we obtain the exact solutions as solution A,

$$\lambda_A = (\sigma/2)\log[\tau_1(1+F_{obs}-\sigma)/\tau_0(1-F_{obs}+\sigma)]^{1/2},$$
$$\rho_0 = (1+F_{obs}-\sigma)/2, \quad \rho_1 = (1-F_{obs}+\sigma)/2, \quad (14)$$

and solution B,

$$\lambda_B = (\sigma/2)\log[\tau_0(1-F_{obs}-\sigma)/\tau_1(1+F_{obs}+\sigma)]^{1/2},$$
$$\rho_0 = (1+F_{obs}+\sigma)/2, \quad \rho_1 = (1-F_{obs}-\sigma)/2. \quad (15)$$

Since (13) is a second-order formula with respect to ρ_k, this model has two analytical solutions. One corresponds to the maximum and the other to the minimum of H. Which solution yields the maximum depends on the magnitude of the prior density and the sign of F_{obs}. If we assume that prior densities are uniform and F_{obs} has a positive value, then solution A becomes the maximum and solution B the minimum.

A relation between the exact solutions and the related functions used to derive the ME equations is shown in Fig. 2 plotted against ρ_0. The selected functions are the entropy function, S, the constraint function multiplied by $-\lambda$, $-\lambda C$, and the summation of these functions, $H' = S - \lambda C$. In the present case, the exact solutions appear on the right-hand side of the prior density. If the prior density is chosen on the right-hand side of the exact solutions, the maximum and the minimum will be exchanged. In all cases, the maximum-entropy solution locates nearer to the prior density. The function S has a single maximum, which occurs at the prior density. The function $-\lambda C$ also has a single maximum, at the midpoint of the exact solutions. Therefore, the function H' becomes a single convex function. In general, it can be shown that H' has a single maximum, since a unique solution should be derived from $\partial H'/\partial \rho_k = 0$. The maximum of H' depends on the value of λ. If the exact λ value, λ_A, is substituted into this function, the maximum appears on the exact solution A in this figure. In a realistic case, the exact λ value is never known. The real problem that arises is how to solve the ME equations without knowing the exact λ value.

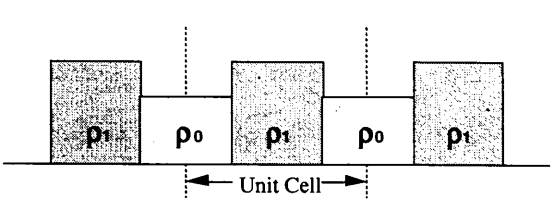

Fig. 1. A schematic picture of a one-dimensional two-pixel crystal model.

4. Computer simulation

With the assumption that $F_{obs} = 0.5$ and $\sigma = 0.1$ in the one-dimensional two-pixel model, a computer simulation was carried out to solve the ME equation without knowledge of the exact λ value. The analytical solution for these values is given by (14) as $\lambda_A = 0.021$, $\rho_0 = 0.7$ and $\rho_1 = 0.3$. In the simulation, (7) is iteratively solved in two different ways. One way is to ignore the ZSPA in order to solve (7), which is equivalent to ignoring the second term of (9). This procedure is called the ZSPA calculation. In the present simple case, (7) can also be solved by a similar kind of iteration including the second term of (9) even when the exact λ value is not known. This is the alternative to the ZSPA and is called the numerical calculation in this paper. In the end, there will be three solutions, the analytical, ZSPA and numerical solutions, for the present one-dimensional two-pixel model.

In order to examine the calculation of each cycle of the iteration, both the ZSPA and the numerical solution are shown in Fig. 3 for three different λ values after the first cycle of the iteration. The solid

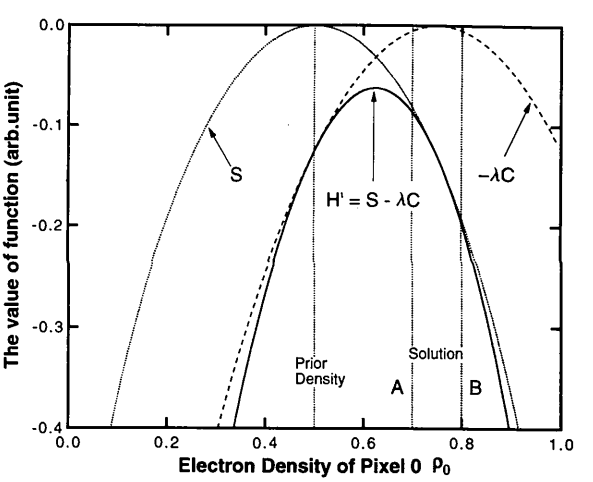

Fig. 2. The entropy function, S, the constraint function multiplied by $-\lambda$, $-\lambda C$, and the summation of these functions, $H' = S - \lambda C$, as functions of ρ_0. The prior density and the exact solutions A and B are also shown.

line is the absolute value of H' as a function of ρ_0, the circles are the numerical solution and the squares are the ZSPA calculation after the first iteration. Since the numerical calculation does not ignore the second term of (9), the obtained value appears on the maximum of H'. The iterative calculations shown by circles and squares in the figure depend very much on λ. As λ becomes bigger, both of the iterative calculations become much more different from the prior density τ_0. The discrepancy between the ZSPA and numerical calculations also depends on λ. As λ becomes bigger, the discrepancy also becomes bigger. At this stage, it cannot be said whether the iteration using that specific λ value converges or diverges.

The difference between the ZSPA and numerical calculations is in the consideration of the second term of (9). The contribution to a part of the second-order derivatives for this term is given by

$$\partial^2 C/\partial\rho_k\partial\rho_{k'} \propto \sum_{j=1}^{M} (1/\sigma_j^2)\exp[2\pi i\mathbf{h}_j(\mathbf{r}_k+\mathbf{r}_{k'})]. \quad (16)$$

Since this term is independent of ρ_k and λ, it can be treated as a constant value. The second term of (9) might be regarded as proportional to $\rho_k - \tau_k$. This explains the λ dependence of the discrepancy between the ZSPA and the numerical calculations. It should be emphasized for the justification of the ZSPA that it is possible to make the discrepancy insignificantly small by choosing a sufficiently small λ value.

The whole iteration process to solve the ME equation is shown in Fig. 4 for both the ZSPA and numerical calculation cases. In the case where $\lambda = 0.001$, both the ZSPA and numerical solutions converged at the exact solution, as shown in Fig. 4(*a*). The difference appeared only in the number of iterations required to reach the exact solution. It took 16

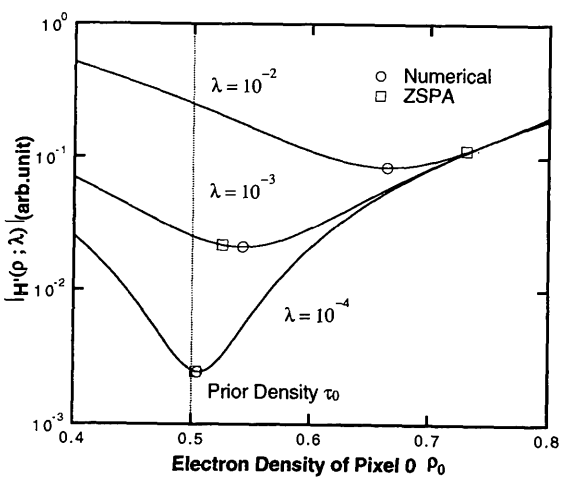

Fig. 3. The ZSPA and the numerical solutions after the first iteration with respect to three different λ values.

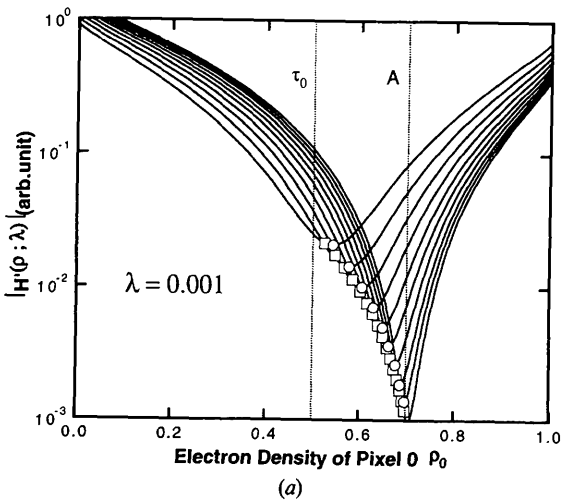

(*a*)

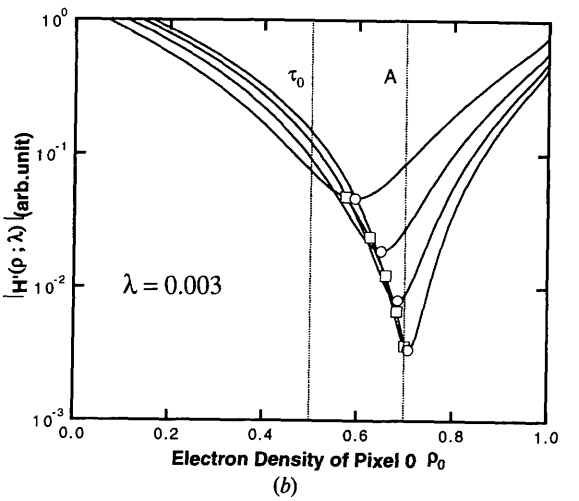

(*b*)

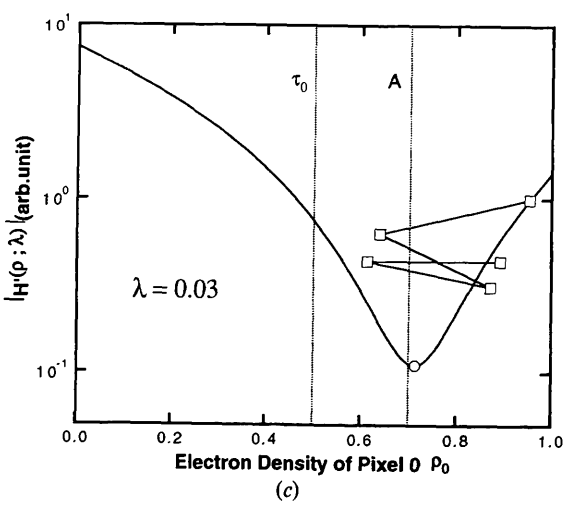

(*c*)

Fig. 4. The ZSPA and the numerical solutions up to convergence or divergence for (*a*) $\lambda = 0.001$, (*b*) $\lambda = 0.003$ and (*c*) $\lambda = 0.03$. The circles represent the numerical solution and the squares the ZSPA solution.

and 19 cycles for the ZSPA and numerical cases, respectively. When $\lambda = 0.003$, the situation is very similar to the previous case shown in Fig. 4(*b*). Both solutions, ZSPA and numerical, converged at the exact solution. The number of iterations was five and four for the ZSPA and numerical cases, respectively, much less than in the previous case. In the case where $\lambda = 0.03$, shown in Fig. 4(*c*), the situation becomes entirely different from the previous two cases. In this case, the λ value exceeds the exact value, 0.021. The numerical calculation converges after only one iteration but to a different value from the exact solution, because the λ value is not the exact value. In the ZSPA case, the iterative solution shows oscillatory behavior and eventually diverges. Therefore, the ME equation cannot be solved by the ZSPA in such a case. This is due to the big difference between the ZSPA and the numerical calculation for such a big λ value. From the practical viewpoint, the case with such a big λ value is not important because a smaller λ can be chosen without any difficulty if there is any doubt about the λ value. It may be emphasized that, whenever the ZSPA converges, it converges at the exact solution. This may be an advantage of ZSPA from the practical viewpoint.

5. Choosing the value of the Lagrange undetermined multiplier

By the computer simulation for the one-dimensional two-pixel model where the exact solution is known, it is understood that the ME equation can be solved by the ZSPA without knowledge of the exact value of λ. There remains the problem of how to choose an appropriate λ that leads to fast and stable convergence. From the practical viewpoint, this is not really a problem apart from with respect to computation time, because choosing the smaller value is always safer when solving the ME equation by the ZSPA. It is still interesting to discuss how to choose the most appropriate λ that gives the fastest convergence.

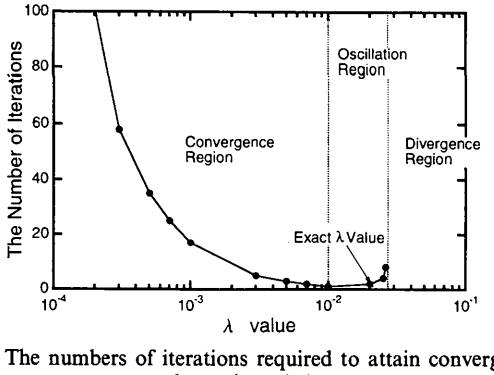

Fig. 5. The numbers of iterations required to attain convergence when λ is varied.

For that purpose, the ME equation for the one-dimensional two-pixel crystal model is solved with various λ values. In Fig. 5, the number of iterations required to reach convergence by the ZSPA is plotted as a function of λ. From the figure, the regions of λ values may be divided into three. When λ is smaller than 0.01, the convergence was attained by monotonic decreasing of the constraint function. In this region, the number of iterations decreases as λ increases. As λ exceeds 0.01, the number of iterations increases again until λ reaches 0.029. In this region, the constraint function does not monotonically decrease and show oscillatory behavior. Once λ exceeds a critical value, *i.e.* 0.029 in this case, the ZSPA does not give convergence. The fastest convergence was obtained at the boundary between monotonic and oscillatory decreasing of the constraint function. This value is less than the exact λ value. It appears here again that the ZSPA solution converges at the exact solution of the ME equation whenever it converges. Though the number of iterations changes depending on λ, the ZSPA solution is independent of the choice of λ. This situation is exactly same as in the radio- and X-ray-astronomy fields (Gull & Daniel, 1978) and the practical three-dimensional electron-density case (Sakata, Mori, Kumazawa, Takata & Toraya, 1990). The solution of each cycle depends on λ, since the solution is derived from (7). But, when the convergence is attained, the final solution does not depend on λ. As the iteration cycles progress near the convergence, the constraint functions decrease very slightly. The difference of ρ_k and τ_k also becomes very small. In such a case, the solution also does not depend on λ, even if λ is increased.

6. Concluding remarks

The validity of the ZSPA was examined by solving the ME equation for a one-dimensional two-pixel model, for which the exact solution is analytically derived. As a simulation of a practical case, an attempt was made to solve the equation iteratively by the ZSPA without knowledge of the exact value of the Lagrange undetermined multiplier λ. It is not guaranteed that the iteration always converges. Whether it converges or diverges depends on λ. When λ exceeds a critical value, it always diverges. If λ is smaller than the critical value, it converges. Whenever the convergence was attained, the ZSPA solution was always equal to the exact solution of a one-dimensional two-pixel model. Since the ZSPA solution does not depend on λ, there is no need to know the critical value. It is very easy to choose an appropriate λ that gives a stable convergence. From the practical viewpoint, the introduction of the

ZSPA presents no problems for the solution of the ME equation. The influence on the ME density map of the introduction of the ZSPA is insignificant.

References

BRICOGNE, G. & GILMORE, C. J. (1990). *Acta Cryst.* A**46**, 284–297.
COLLINS, D. M. (1982). *Nature (London)*, **298**, 49–51.
GILMORE, C. J., BRICOGNE, G. & BANNISTER, C. (1990). *Acta Cryst.* A**46**, 297–308.
GULL, S. F. & DANIEL, G. J. (1978). *Nature (London)*, **272**, 686–690.
SAKATA, M., MORI, R., KUMAZAWA, S., TAKATA, M. & TORAYA, H. (1990). *J. Appl. Cryst.* **23**, 526–534.
SAKATA, M. & SATO, M. (1990). *Acta Cryst.* A**46**, 263–270.
SAKATA, M., UNO, T., TAKATA, M. & HOWARD, C. J. (1993). *J. Appl. Cryst.* **26**, 159–165.
SAKATA, M., UNO, T., TAKATA, M. & MORI, R. (1992). *Acta Cryst.* B**48**, 591–598.
WILKINS, S. W., VARGHESE, J. N. & LEHMANN, M. S. (1983). *Acta Cryst.* A**39**, 47–60.

Acta Cryst. (1995). A**51**, 53–60

A New Commensurate Modulated Structure in Orthoclase

BY HUIFANG XU*

Department of Earth and Planetary Sciences, The Johns Hopkins University, Baltimore, Maryland 21218, *USA, and Department of Earth Sciences, Nanjing University, Nanjing, Jiangsu* 210008, *People's Republic of China*

DAVID R. VEBLEN

Department of Earth and Planetary Sciences, The Johns Hopkins University, Baltimore, Maryland 21218, *USA*

AND GUFENG LUO

Department of Earth Sciences, Nanjing University, Nanjing, Jiangsu 210008, *People's Republic of China*

(*Received* 2 *April* 1994; *accepted* 9 *June* 1994)

Abstract

Transmission electron microscopy shows that there is an ordered modulated structure in orthoclase ($Or_{84.6}Ab_{13.1}An_{2.3}$) (Or = orthoclase, Ab = albite, An = anorthite) of an augite monzonite from Wulian, Shandong Province, Northern China. The modulated orthoclase is composed of a series of triclinic (010) layer domains with $C\bar{1}$ symmetry. Each domain has a thickness of $4d_{010}$ and the domains are periodically arranged along the b axis. The modulation period along the b axis is thus 104 Å ($=8d_{010}$). The relationship between the extended unit-cell parameters of the modulated structure (supercell) and the triclinic subcell parameters is: $a_{sup} \simeq a_{sub}$; $b_{sup} = 8d_{010} \simeq 8b_{sub}$; $c_{sup} \simeq c_{sub}$; $\beta_{sup} \simeq \beta_{sub}$. The probable space group of the commensurately modulated orthoclase is Pm. The modulated structure probably forms during the phase transition from sanidine ($C2/m$ symmetry) to microcline ($C\bar{1}$ symmetry) through the segregation of Al atoms from T_2 sites into $T_{1(0)}$ and $T_{1(m)}$ sites, respectively, in neighboring domains, which are in the albite-twin relationship. The ordering of Al atoms in the tetrahedral sites during the phase transition results in a sinusoidal deviation of the crystal structure from monoclinic symmetry. The Al–Si distribution near the domain boundary positions is likely to be relatively disordered.

1. Introduction

In structure, orthoclase [$(K,Na)AlSi_3O_8$] can be considered to be a heterogeneous crystal composed of domains with triclinic symmetry. The twins are so fine in scale that experiments using light or X-rays indicate only an average monoclinic ($C2/m$) average structure, rather than the local triclinic ($C\bar{1}$) symmetry of the individual domains (Smith, 1974; Laves, 1950; Goldsmith & Laves, 1954). Orthoclase is generally considered to be a metastable phase between sanidine and microcline and represents a stage in the ordering of aluminium in the tetrahedral sites of potassium feldspar (Smith, 1974; Laves, 1950; Goldsmith & Laves, 1954; Ribbe, 1983). The ordering of aluminium and silicon in the tetrahedron sites, exsolution microstructures and tweed textures in alkali feldspars have been thoroughly studied both theoretically and experimentally (Ribbe, 1983;

* Author for correspondence. Present address: Department of Geology, Arizona State University, Tempe, Arizona 85287, USA.